Breakdown of the adiabatic approximation in *trans*-polyacetylene

William Barford,[1,*] Robert J. Bursill,[2,†] and Mikhail Yu Lavrentiev[1,‡]
[1]*Department of Physics and Astronomy, The University of Sheffield, Sheffield, S3 7RH, United Kingdom*
[2]*School of Physics and Astronomy, The University of New South Wales, Sydney, NSW 2052, Australia*
(Received 20 January 2000; published 22 January 2002)

We solve a model of interacting electrons coupled to longitudinal phonons using the density matrix renormalization group method. The model is parametrized for *trans*-polyacetylene. We calculate the ground state and first excited odd-parity singlet and triplet states. We investigate their energies and geometries for up to 102 sites. The transition energy and the soliton width of the triplet state show significant deviations from the adiabatic approximation for chain lengths larger than the classical soliton size. In contrast, the transition energy of the singlet is close to the adiabatic prediction.

DOI: 10.1103/PhysRevB.65.075107 PACS number(s): 71.20.Rv, 63.20.Kr

I. INTRODUCTION

The interplay of electron-electron interactions and electron-lattice coupling in polyene oligomers and *trans*-polyacetylene, $(CH)_x$, results in a rich variety of low-energy excitations. These excitations include triplet states of soliton-antisoliton pairs, singlet states comprising bound pairs of triplets, and exciton-polarons. Within the adiabatic (or semiclassical) approximation[1] the nature and energy of these excitations are now fairly well understood. A realistic model of π-conjugated systems (the Pariser-Parr-Pople-Peierls model), solved within the adiabatic approximation, predicts accurate excitation energies for oligomers of up to 20 or so sites.[2,3] However, for longer chains the calculations deviate from the experimental polyacetylene thin film results. These discrepancies are partly explained by the self-trapping (or localization) of the excited states by the lattice:[4] the calculated energies deviate from a linear extrapolation in the inverse chain length as the chain length becomes larger than the solitonic structures. Furthermore, a linear extrapolation in the inverse chain length of the oligomer experimental values predicts infinite chain energies of the dipole-allowed singlet $(1\,^1B_u^-)$ and the dipole-forbidden singlet $(2\,^1A_g^+)$ close to those observed in polyacetylene thin films,[5] suggesting that self-trapping may be a partial artifact of the adiabatic approximation.[6]

The question therefore remains as to the role of quantized lattice fluctuations on the depinning (or delocalization) of the excited states. These fluctuations are the subject of this paper. Our key results are that the depinning of some excited states due to quantum lattice fluctuations is significant as the conjugation length increases. In particular, there is a significant reduction in the energy and an associated increase in the soliton width of the triplet state, indicating a breakdown of the adiabatic approximation for the low-lying spin density wave states. These quantum corrections go a long way towards removing the discrepancies between the calculated semiclassical excitation energies and the experimental thin film results.

There have been a number of studies of quantized lattice dynamics in the ground state of the uncorrelated Su-Schrieffer-Heeger model,[7] indicating that fluctuations in the bond length are comparable to the bond length changes, but that the Peierls dimerization is stable against such fluctuations. There has also been a variational Monte Carlo study of an interacting electron-phonon model.[8] However, there have been no studies of excited states, as the incorporation of quantized lattice dynamics into the correlated Pariser-Parr-Pople-Peierls model presents a formidable challenge.

The advent of the density matrix renormalization group (DMRG) method[9,10] has enabled definitive model studies of correlated electron systems, including long-range interactions[2,3,11] and dynamical phonons.[12,13] In this work we report the results of extensive calculations on a realistic model system which affords us insight into the effect of quantized lattice dynamics on the properties of excited states of long polyenes. The model and the DMRG method are discussed in Secs. II and III, respectively. In Sec. IV we discuss our results, concluding in Sec. V.

II. THE MODEL

π electrons, interacting via long-range Coulomb forces, are coupled to longitudinal phonons. The electrons couple to the phonons in two ways. First, changes in bond length are assumed to lead to linear corrections to the hybridization integrals. Second, changes in bond lengths also affect the Coulomb interactions. In order to quantize these fluctuations, we linearize the deviations in the Coulomb interaction. We retain only nearest neighbor deviations to the Coulomb interaction, so that we may compare our quantized results to the semiclassical Hellmann-Feynman calculation.[3]

The Hamiltonian is thus defined as,[13,3]

$$\begin{aligned}\mathcal{H}=&\hbar\omega\sum_{i=2}^{N-1}\left(b_i^\dagger b_i+\frac{1}{2}\right)-\hbar\omega\sum_{i=1}^{N-1}B_{i+1}B_i+U\sum_{i=1}^{N}\left(N_{i\uparrow}-\frac{1}{2}\right)\\&\times\left(N_{i\downarrow}-\frac{1}{2}\right)+\frac{1}{2}\sum_{i\neq j}^{N}V_{ij}(N_i-1)(N_j-1)\\&-t\sum_{i=1,\sigma}^{N-1}[1-g(B_{i+1}-B_i)](c_{i+1\sigma}^\dagger c_{i\sigma}+c_{i\sigma}^\dagger c_{i+1\sigma})\\&-W\sum_{i=1}^{N-1}(B_{i+1}-B_i)(N_i-1)(N_{i+1}-1).\end{aligned}\tag{1}$$

TABLE I. The ground state ($1\,^1A_g^+$) and triplet ($1\,^3B_u^+$) energies (eV) as a function of the number of optimized states per site for the 30-site chain with five bare phonons per site (i.e., 24 bare electron-phonon states per site).

Optimized states	$E(1\,^1A_g^+)$	$E(1\,^3B_u^+)$	$E(1\,^3B_u^+)-E(1\,^1A_g^+)$
10	−149.4647	−148.7655	0.6992
14	−149.5331	−148.8477	0.6854
18	−149.5428	−148.8564	0.6844

$b_i^\dagger$ (b_i) creates (destroys) a phonon and $c_{i\sigma}^\dagger$ ($c_{i\sigma}$) creates (destroys) an electron on site *i*. $B_i=(b_i^\dagger+b_i)/2$, $g=(\lambda\pi\hbar\omega/2t)^{1/2}$, and $\omega=\sqrt{2}\omega_0=\sqrt{2K/m}$. We use the Ohno function for the Coulomb interaction, $V_{ij}=U/\sqrt{1+\beta r_{ij}^2}$, where the bond lengths are in Å and $\beta=(U/14.397)^2$. The undistorted bond length (a_0) used in the evaluation of V_{ij} is 1.40 Å , and the bond angle is 120°. $W=(\hbar\omega/K)^{1/2}U\beta a_0/(1+\beta a_0^2)^{3/2}$, $t=2.539$ eV, $U=10.06$ eV, $\lambda=0.1$,[2] $\hbar\omega_0=0.2$ eV,[14] and $K=46$ eV Å^{-2}.[16] Fixed chain lengths are enforced by having no phonon degrees of freedom on the end sites. In the absence of electron-phonon coupling, Eq. (1) is the undimerized Pariser-Parr-Pople model, while in the semiclassical limit it is the Pariser-Parr-Pople-Peierls model.

We intend to compare our quantum treatment of the lattice to the semiclassical limit, where the classical displacements $q_i=(\hbar\omega/K)^{1/2}\langle B_i\rangle$ are found by the Hellmann-Feynman theorem. To do this, we set $\omega=0$ in Eq. (1), and supplement $\mathcal{H}$ by

$$\mathcal{H}'=\Gamma(2\pi t\lambda K)^{1/2}\sum_{i=1}^{N-1}(q_{i+1}-q_i), \tag{2}$$

where Γ is determined by the requirement that the chain length remains constant.[3]

III. THE DMRG METHOD AND CONVERGENCE TESTS

The essential approach we adopt to solve Eq. (1) is an extension of the local Hilbert space reduction of Ref. 15 for a single site. The bare electron-phonon Hilbert space for a single site consists of $4\times$(number of bare phonons per site $+1$) states. For more than three or four bare phonons there are too many single-site states to augment with the system block; thus an optimal truncation is required. The optimal electron-phonon basis is found by constructing a reduced density matrix for this site by tracing over the states of the remaining three blocks (the system and environment blocks, and the adjacent site). The full electron-phonon Hilbert space is used for the target site. The optimal states are then the density matrix eigenstates with the largest eigenvalues.

Once a single-site Hilbert space is optimized it is then augmented with the system block in the standard finite lattice algorithm.[9] Since the classical lattice geometry of excited states changes as the chain length increases, there is no *a priori* reason to suppose that the optimal site electron-phonon basis for the shortest chain is appropriate for longer chains. Thus, it is generally necessary to perform *in situ* optimization: a site Hilbert space is reoptimized when it forms part of the target chain size. Generally, we expect *in situ* optimization to be necessary whenever the short scale properties are modified by the long scale properties. During the *in situ* optimization only a few states (typically 80) are retained for the system and environment blocks, while typically, 160 states are used for the system and environment blocks during augmentation. A further truncation parameter is the product of the density matrix eigenvalues, ϵ, of the four single block states used in the tensor product to construct a superblock state. Only superblock states with an ϵ greater than the cutoff are retained in the superblock Hilbert space.[17]

A key goal of this work is to study excited states, which we do by exploiting the particle-hole ($\hat{J}$) and spin-flip ($\hat{P}$) symmetries of Eq. (1). The inversion symmetry is measured at the middle of a finite lattice sweep. We have checked that setting $J=+1$ and $P=+1$ targets the ground ($1\,^1A_g^+$) state, setting $J=-1$ and $P=+1$ targets the $1\,^1B_u^-$ state, and setting $J=+1$ and $P=-1$ targets the triplet ($1\,^3B_u^+$) state.

We now turn to the convergence tests. These tests were performed at up to 30 sites, because at this chain length significant deviations between the quantum and semiclassical calculations are evident. We first establish convergence with respect to the number of optimized states per site. Table I shows the ground state and triplet energies for the 30-site chain with five bare phonons per site. We see that with 18 states the transition energy has converged to within 0.001 eV. Next, we consider the convergence with superblock Hilbert space size at 30 sites. As shown in Table II, the convergence of the ground state energy is reasonable for up to 180 000 states, and the transition energy has converged to better than 0.01 eV. Finally, we consider the triplet transition energy as a function of the number of bare phonons per site for various

TABLE II. The ground state ($1\,^1A_g^+$) and triplet ($1\,^3B_u^+$) energies (eV) as a function of the density matrix eigenvalue product cutoff (ϵ_c), the number of system block states (m), and superblock Hilbert space size (SBHSS) for the 30-site chain with five bare phonons per site. There are 18 optimized states per site.

ϵ_c	$1\,^1A_g^+$			$1\,^3B_u^+$			$E(1\,^3B_u^+)-E(1\,^1A_g^+)$
	m	SBHSS	$E(1^1A_g^+)$	m	SBHSS	$E(1^3B_u^+)$	
10^{-12}	79	54876	−149.5377	103	102770	−148.8456	0.6921
10^{-13}	110	105640	−149.5417	124	178568	−148.8528	0.6889
10^{-14}	131	180568	−149.5428	145	304896	−148.8584	0.6844
10^{-14}	150	200226	−149.5432	182	410984	−148.8614	0.6818

TABLE III. The triplet transition energies (eV) as a function of the number of sites, N. The model [Eq. (1)] with zero phonons is the undimerized Pariser-Parr-Pople model.

N	Number of bare phonons per site						Semiclassical
	0	1	2	3	4	5	
6	1.8075	1.9259	1.9631	1.9751	1.9789	1.9799	2.0261
14	0.8616	1.0200	1.0648	1.0796	1.0860	1.0887	1.1923
30	0.4212	0.5917	0.6518	0.6712	0.6800	0.6844	0.8842
50	0.2559	—	0.5306	—	—	0.5578	0.8500
66	0.1935	—	0.4949	—	—	—	0.8494
82	0.1541	—	0.4790	—	—	—	0.8490
102	0.1209	—	0.4718	—	—	—	0.8486

chain lengths, as shown in Table III. We see that the transition energy has converged to better than 0.01 eV with five phonons per site. We conclude from the convergence tests that by using five bare phonons and 18 optimal states per site and ca. 160 states per system block, the transition energies have converged to better than 0.01 eV. We use these parameters to extend the quantum calculations to 50 sites. As the chain length increases, however, these calculations become prohibitively expensive in computer time. For chain lengths of greater than 50 sites we retain two bare phonons per site. The convergence of the transition energies at 50 sites with respect to the number of bare phonons suggests that the energies are still accurate to much better than 0.1 eV.

IV. RESULTS AND DISCUSSIONS

Figure 1 shows the transition energies for the $1\,^1B_u^-$ and $1\,^3B_u^+$ states as a function of inverse chain length for up to 102 sites. For short chains the differences between the transition energies in the quantum and semiclassical limits are very small. However, the quantum calculation of the triplet state energy deviates from the semiclassical result in two ways. First, the gradient as a function of inverse chain length is greater, and second, the flattening off of the energy occurs at a larger chain length. As a consequence, there is a clear deviation between these limits for the triplet state as the conjugation length increases. This deviation is a result of the depinning of the excited state by the lattice fluctuations. In contrast, the deviation between the semiclassical and quantum limits for the singlet excited state is relatively modest. At 50 sites, using five bare phonons, the deviations are 0.29 eV and 0.07 eV for the triplet and singlet states, respectively, while at 102 sites, using two bare phonons, the deviations are 0.38 eV and 0.14 eV for the triplet and singlet states, respectively.

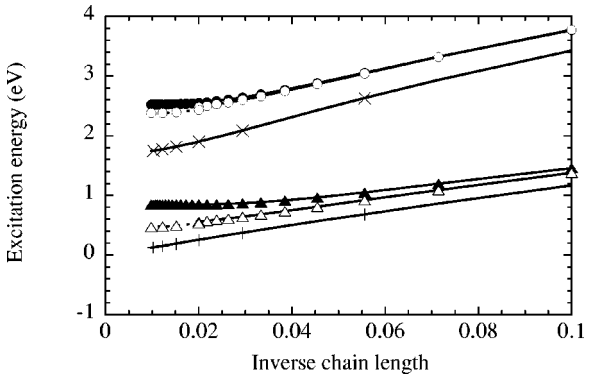

FIG. 1. Transition energies for the $1\,^1B_u^-$ (circles) and $1\,^3B_u^+$ (triangles) states as a function of inverse chain length. Semiclassical (quantum) calculations are indicated by solid (open) symbols. The quantum calculations for five (10 to 50 sites) and two (50 to 102 sites) bare phonons per site are shown by solid and dashed lines, respectively. Also shown are the $1\,^1B_u^-$ ($\times$) and $1\,^3B_u^+$ ($+$) transition energies for the undimerized Pariser-Parr-Pople model [i.e., Eq. (1) with zero phonons, or equivalently the limit $\hbar\omega\rightarrow\infty$].

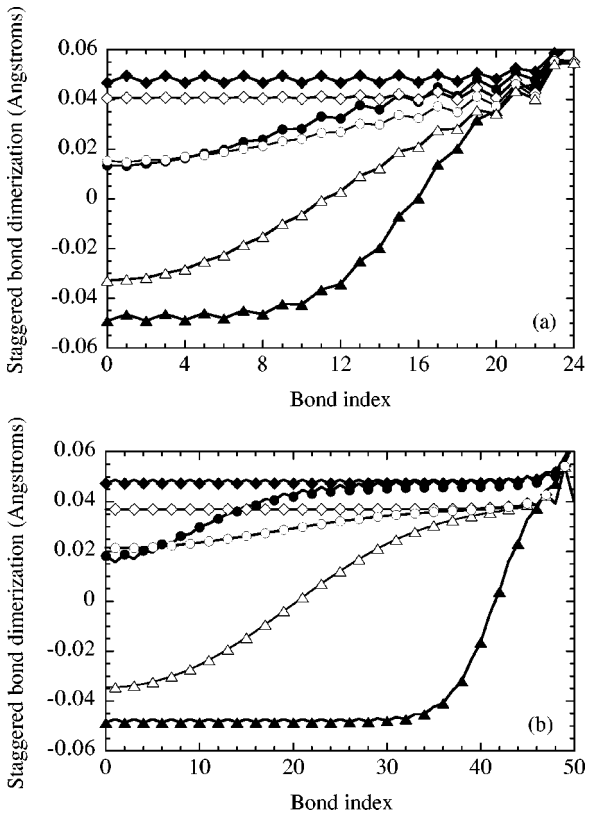

FIG. 2. The geometries (staggered bond distortion as a function of bond index from the center of the chain) of various states: $1\,^1A_g^+$ (diamonds), $1\,^1B_u^-$ (circles), and $1\,^3B_u^+$ (triangles). Semiclassical (quantum) calculations are indicated by solid (open) symbols. (a) 50-site chain with five bare phonons per site in the quantum calculation. (b) 102-site chain with two bare phonons per site in the quantum calculation.

Further insight into the depinning of the excited states can be obtained from a study of their geometrical structures. We calculate the classical phonon displacement, q_i, the bond length distortion, and the root-mean-square fluctuations in the bond length. Figure 2(a) shows the staggered bond length changes in the ground state and excited states of a 50-site chain. We see that the ground state dimerization of ca. 0.04 Å in the quantum limit is slightly smaller than the semiclassical result of ca. 0.05 Å . We find that in the limit of long chains the relative root-mean-square fluctuation in the bond

TABLE IV. The triplet transition energies (eV) as a function of the phonon energy at 30 sites. In the limit that $\hbar\omega_0 \to \infty$ the model [Eq. (1)] becomes the undimerized Pariser-Parr-Pople model. Five bare phonons and 18 optimized states per site were used in the quantum calculation.

Pariser-Parr-Pople	Quantum phonons			Semiclassical
	$\sqrt{10}\hbar\omega_0 = 0.632$ eV	$\hbar\omega_0 = 0.2$ eV	$\hbar\omega_0/\sqrt{10} = 0.0632$ eV	
0.4214	0.5257	0.6844	0.8026	0.8842

length is ca. 0.9, almost independent of the number of phonons per site, and close to previous theoretical[7] and experimental[18] estimates.

Significant deviations are found between the quantum and semiclassical predictions for the triplet soliton structures. The soliton width in the semiclassical calculation (ca. 10 bond lengths) is relatively short, and much less than half the chain length at 50 sites. Provided that a soliton is further away than its half-width from another soliton or a chain end, its potential energy varies very weakly with bond index. This explains the location of the solitons near the chain ends in our semiclassical calculation, as our DMRG procedure increases the chain size by inserting new bonds in the center of the chain. The classical soliton structure also pins the electronic wave function, and leads to the flattening off of the triplet transition energy.

In contrast, the soliton width in the quantum limit is greater than half the chain length at 50 sites, and hence the soliton and antisoliton are repelled by each other and by the chain ends. Furthermore, since the chain length has not exceeded twice the soliton width, the electronic wave function is not yet pinned, and the transition energy is still decreasing with chain length. At 102 sites, shown in Fig. 2(b), the soliton width of the triplet in the quantum calculation is roughly half the chain size, and so, as expected the transition energy is fairly flat as function of chain length.

Finally, we consider the optically allowed excitonic ($1\,^1B_u^-$) state. According to the adiabatic approximation,[19] this state creates a shallow polaronic distortion of the lattice, with self-trapping only becoming important for chain lengths longer than ca. 40 sites.[2] This is confirmed by the excitation energies shown in Fig. 1, indicating that the transition energies calculated in the quantum limit are within ca. 0.1 eV of the semiclassical result, and Fig. 2, showing that the quantum and semiclassical polaronic structures are similar (although wider in the quantum calculation).

As already noted in Ref. 1, we should expect our quantum calculation to approach the semiclassical approximation in the limit that $\omega \to 0$. We check this by repeating the calculation for two other values of phonon frequency: $\sqrt{10}\omega_0$ and $\omega_0/\sqrt{10}$. These results, shown in Table IV, indeed show that as ω is reduced the transition energies approach the semiclassical limit. The nature in which the quantum result approaches the semiclassical result as a function of ω is interesting subject, which we discuss briefly in the Conclusions. However, it lies outside the main scope of this paper.

V. CONCLUSIONS

In conclusion, an extended DMRG method has been applied to an interacting electron-phonon model of polyenes. Quantum lattice fluctuations play an important role in the depinning of the self-trapped excited states, leading to corrections to the adiabatic approximation. Corrections to the adiabatic approximation are particularly important for the lowest-lying triplet, as this state is gapless in the long chain limit in the absence of electron-phonon coupling[3] (i.e., the Pariser-Parr-Pople model). Figure 1 and Table III show the triplet transition energy for the undimerized Pariser-Parr-Pople model. Thus, the phonon frequency is not small in comparison to the electronic energy scale, and the approximation of slow nuclear motion relative to the electronic time scales is no longer valid. This breakdown of the adiabatic approximation is an emergent property of long chains. At 102 sites the phonon-calculated triplet energy is only 56% of the adiabatic approximation. Since the dipole-forbidden $2\,^1A_g^+$ state is formed from a pair of bound triplets, this reduction in the triplet energy from quantum fluctuations is also expected to apply to the $2\,^1A_g^+$ state. It would be reasonable to expect that the semiclassical prediction[3] of 1.74 eV for its transition energy might be reduced to ca. 1.0 eV with the inclusion of quantum phonons. This prediction is very close to Kohler's linear extrapolation[5] and to the experimental determination of the $2\,^1A_g^+$ energy by Halverson and Heeger.[20,21]

The reduction of the triplet transition energy is associated with a significant increase in the soliton width. Self-trapping occurs when the chain length exceeds twice the soliton width. As the phonon frequency increases, the model [Eq. (1)] approaches the Pariser-Parr-Pople model (i.e., with no phonons), and the soliton width increases. Furthermore, as the chain length increases the Pariser-Parr-Pople model predicts that the triplet energy tends to zero. Whether or not the Eq. (1) is in the adiabatic limit is determined by a comparison of the excitation energy of the Pariser-Parr-Pople model to the phonon frequency at chain lengths comparable to the soliton width. However, because the soliton width is determined by the phonon frequency, there is no *a priori* way of predicting whether or not the Eq. (1) is in the adiabatic limit. As already stated, this argument suggests that the $2\,^1A_g^+$ state is not in the adiabatic limit for these model parameters, as its

TABLE V. The singlet ($1\,^1B_u^-$) transition energies (eV) as a function of the number of sites, N.

N	Number of bare phonons per site			Semiclassical
	0	2	5	
50	1.9003	2.4341	2.4809	2.5508
102	1.7427	2.3788	—	2.5211

energy is also gapless in the long-chain limit of the Pariser-Parr-Pople model.

In contrast, the exciton-polaron ($1\,^1B_u^-$) state is expected to be in the adiabatic limit, as its energy in the Pariser-Parr-Pople model is 1.6 eV in the long-chain limit.[3] This is confirmed by the current calculation, and in particular Fig. 1 and Table V, which show that the deviations between the quantum and semiclassical limits is only ca. 0.1 eV at 102 sites.

In this paper we claim that quantum corrections to the adiabatic approximation lead to the delocalization of the low-lying spin-density wave states. However, a further contribution to this delocalization may be interchain coupling. A rigorous analysis of the effects of interchain coupling within the present model lies outside the scope of the current paper.

ACKNOWLEDGMENTS

This work was supported by the EPSRC (U.K.) (GR/K86343 and GR/R03921), the Royal Society, the Australian Research Council, and the J.G. Russell Foundation.

*Email address: W.Barford@sheffield.ac.uk

†Email address: ph1rb@phys.unsw.edu.au

‡Current address: The School of Chemistry, University of Bristol, Bristol, U.K. On leave from Institute of Inorganic Chemistry, 630090 Novosibirsk, Russia. Email address: M.Lavrentiev@bristol.ac.uk

[1] The kinetic energy of the atoms is ignored in the adiabatic approximation. The atoms are treated classically, while the electrons are treated quantum mechanically. In principle, the adiabatic approximation is the limit that the phonon frequency $\rightarrow 0$ and the number of phonons per site $\rightarrow \infty$, but see Ref. 6.

[2] R. J. Bursill and W. Barford, Phys. Rev. Lett. **82**, 1514 (1999).

[3] W. Barford, R. J. Bursill, and M. Yu. Lavrentiev, Phys. Rev. B **63**, 195108 (2001). be published).

[4] For the optically allowed ($1\,^1B_u^-$) excitation there is an additional correction due to the polarization of the surrounding medium of a few tenths of an eV for all chain lengths [E. Moore, B. Gherman, and D. Yaron, J. Chem. Phys. **106**, 4216 (1997)].

[5] B. E. Kohler, J. Chem. Phys. **88**, 2788 (1988).

[6] Fisher and Zwerger [M. P. A. Fisher and W. Zwerger, Phys. Rev. B **34**, 5912 (1986)] have argued that for the ground state of the polaron problem ''the self-trapping transition found in the adiabatic approach is an artefact of the approximations used.''

[7] W. P. Su, Solid State Commun. **42**, 497 (1982); E. Fradkin and J. H. Hirsch, Phys. Rev. B **27**, 1680 (1983).

[8] B. J. Alder, K. J. Runge, and R. T. Scalettar, Phys. Rev. Lett. **79**, 3022 (1997).

[9] S. R. White, Phys. Rev. Lett. **69**, 2863 (1992).

[10] Density Matrix Renormalization, edited by I. Peschel, X. Wang, M. Kaulke, and K. Hallberg (Springer, Berlin, 1999).

[11] D. Yaron, E. E. Moore, Z. Shuai, and J. J. Bredas, J. Chem. Phys. **108**, 7451 (1998); G. Fano, F. Ortolani, and L. Ziosi, *ibid.* **108**, 9246 (1998).

[12] L. G. Caron and S. Moukouri, Phys. Rev. Lett. **76**, 4050 (1996); E. Jeckelmann and S. R. White, Phys. Rev. B **57**, 6376 (1998); R. J. Bursill, R. H. McKenzie, and C. J. Hamer, Phys. Rev. Lett. **80**, 5607 (1998); **83**, 408 (1999); E. Jeckelmann, C. Zhang, and S. R. White, Phys. Rev. B **60**, 7950 (1999); C. Zhang, E. Jeckelmann, and S. R. White, *ibid.* **60**, 14 092 (1999).

[13] L. G. Caron and S. Moukouri, Phys. Rev. B **56**, R8471 (1997).

[14] F. B. Schugerl and H. Kuzmany, J. Chem. Phys. **74**, 953 (1981).

[15] C. Zhang, E. Jeckelmann, and S. R. White, Phys. Rev. Lett. **80**, 2661 (1998).

[16] E. Ehrendfreund *et al.*, Phys. Rev. B **36**, 1535 (1987).

[17] R. J. Bursill, Phys. Rev. B **60**, 1643 (1999).

[18] R. H. McKenzie and J. W. Wilkin, Phys. Rev. Lett. **69**, 1085 (1992).

[19] M. Grabowski, D. Hone, and J. R. Schrieffer, Phys. Rev. B **31**, 7850 (1985).

[20] C. Halverson and A. J. Heeger, Chem. Phys. Lett. **216**, 488 (1993).

[21] S. Mazumdar has pointed out that the apparent nonlinear optical absorption associated with the $2\,^1A_g^+$ may instead be due to linear absorption to charged solitons (private communication).